

## Article

# Study on the Microstructure Evolution and Strength Deterioration of Powder Crystal Dolomite under Dissolution

Wenlian Liu <sup>1</sup>, Feng Ji <sup>2,\*</sup>, Pengen Liu <sup>2</sup>, Hanhua Xu <sup>1</sup> and Xiansen Meng <sup>2</sup>

<sup>1</sup> Kunming Prospecting Design Institute of China Nonferrous Metals Industry, Kunming 650051, China; liuwenlian@zskk1953.com (W.L.); xuhanhua@cug.edu.cn (H.X.)

<sup>2</sup> State Key Laboratory of Geohazard Prevention and Geo-Environment Protection, Chengdu University of Technology, Chengdu 610059, China; 2021020334@stu.cdut.edu.cn (P.L.); 2021050253@stu.cdut.edu.cn (X.M.)

\* Correspondence: 2021050228@stu.cdut.edu.cn; Tel.: +86-17866535823

**Abstract:** To study the influence of water–rock interactions on the deterioration of rock, particularly the problems of the complex dissolution mechanism of dolomite and the difficulty in establishing chemical damage, dolomite obtained from a tunnel in Yuxi City was utilized. The macroscopic and microscopic dissolution characteristics of dolomite were analyzed using an indoor dissolution test combined with the hydrochemical characteristics of the study area, which were found to be favorable for dissolution. The dissolution of dolomite indicates the chemical decomposition of dolomite crystals, and the crystal failure mode is divided into intergranular dissolved pores and intracrystalline micropore development. Under various pH conditions, as H<sup>+</sup> is immersed in the rock sample, the failure mode of the rock sample develops from longitudinal cracks to transverse and longitudinal staggered cracks. Based on the aforementioned conclusions, in addition to the principle of chemical kinetics and the generalized Lemaitre strain equivalence principle, a damage model suitable for dolomite chemical erosion was defined. The fitting degree between the calculated value of uniaxial compressive strength and the experimental value reaches 98%, which is of excellent prediction accuracy and reliability. The model for dolomite chemical damage proposed herein provides a theoretical basis for dolomite dissolution damage; the theory of rock chemical damage is thereby enhanced.

**Keywords:** dolomite; indoor dissolution test; dissolution characteristics; chemical injury; damage model



**Citation:** Liu, W.; Ji, F.; Liu, P.; Xu, H.; Meng, X. Study on the Microstructure Evolution and Strength Deterioration of Powder Crystal Dolomite under Dissolution. *Water* **2024**, *16*, 1989. <https://doi.org/10.3390/w16141989>

Academic Editors: Shi Yu and Guanghui Jiang

Received: 20 May 2024  
Revised: 5 July 2024  
Accepted: 9 July 2024  
Published: 13 July 2024



**Copyright:** © 2024 by the authors. Licensee MDPI, Basel, Switzerland. This article is an open access article distributed under the terms and conditions of the Creative Commons Attribution (CC BY) license (<https://creativecommons.org/licenses/by/4.0/>).

## 1. Introduction

The structure of the rock is prone to transform into sand grains of varying sizes upon strong erosion of the dolomite, which are of low strength and can be scattered into sand by manually pinching. This type of karst geological phenomenon is known as dolomitic karst sanding [1]. Karst sanding of dolomite reduces the strength and quality of the rock mass, and forms unfavorable geological boundaries by significantly affecting the stability of slopes and underground chambers. Therefore, exploring the mechanism of dolomite sandification and establishing a model of the damage for rocks under hydrochemical action is theoretically significant [2–4]. Tang et al. [5] proposed the concept of chemical damage and analyzed its mechanism in rock water. They applied the theory of chemical composition analysis, energy viewpoint, and the damage mechanics method to analyze the quantitative method. Wang et al. [6] found that the ionic composition and pH value greatly affect the mechanical properties of red sandstone while using indoor tests. The peak strength, residual strength, and elastic modulus of the rocks decreased by different degrees after dissolution in various chemical solutions. Tang et al. [7] reported the deformation mechanism of rock salt dissolution characteristics under different circumferential pressures through numerous triaxial tests. Wei et al. [8] simulated the effect of aqueous solutions with different pH values on limestone dissolution and established a time-scale relationship

between these solutions. Selective dissolutions exist in the composition and mineralogical composition of the rocks. Tian et al. [9] analyzed the dissolution difference between various carbonates based on a dissolution test of combined with scanning electron microscopy. In the theoretical context of chemical kinetics, Li et al. [10] discussed the chemical reactions between sandstone samples and acidic solutions at different curing temperatures and pressures, as well as their damage mechanisms. Liu et al. [11] discussed the chemical damage mechanism of dolomite from macroscopic and microscopic perspectives using indoor dissolution tests.

While the damage to rock properties caused by different water chemical characteristics has been investigated [12], other studies have actively worked on developing damage models of rocks under different water chemical environments [13]. Li et al. [14] conducted indoor simulations of solutions with various pH levels for textured cemented feldspathic sandstones. A chemical damage strength model was proposed for rocks that could be applied to acidic solutions using the chemical kinetic theory and damage mechanics theory, and the model was tested and validated. Chen et al. [15] conducted an instantaneous scanning test on sandstone under chemical dissolution using a CT identification technique for the entire triaxial loading process. They successfully developed a damage variable model based on the effects of chemical dissolution and CT numbers. Ding et al. [16] analyzed the characteristics of the effects of different chemical solutions on each stage of total stress–strain in tuffs. Qiao et al. [17] combined secondary pore damage with CT scan data to develop a chemical damage model for sandstone. Liu et al. [18] simulated the relationship between the strength and time variation of specimens by modeling the dissolution depth under acidic conditions in sandstone. Deng et al. [19] established a statistical damage constitutive equation for sandstone under the action of water–rock using continuous damage mechanics and statistical theory. Feng et al. [20] analyzed the relationship between pH change with time during the chemical dissolution process and introduced this equation into the chemical damage formula. Additionally, using the creep damage formula, a rheological damage constitutive model of sandstone considering hydrochemical damage was established. Based on the time-softening damage analysis of gypsum rock immersion in laboratory tests, Zhu et al. [21] derived the damage evolution equation of gypsum immersion softening based on the time factor from the perspective of damage mechanics and revealed the relationship between the brittleness coefficient and softening damage variable. Lin et al. [22] considered the damage variable correction coefficient and chemical damage variable determined by porosity to establish a statistical damage model. KUVA J et al. [23] studied the micro-pore structure of rock under different soaking time using X-ray tomography and SEM scanning electron microscopy.

Qualitative and quantitative studies on rock hydrochemical damage and the establishment of damage models are abundant, mainly for sandstone and limestone. Dolomite found specifically in the Sichuan–Yunnan area of China exhibits a strong dissolution effect in water. Therefore, based on this geological environment, this study explores the microscopic mechanism of dolomite dissolution using a dissolution test, electron microscope scanning test, and damage mechanics analyses. A microscopic model of dolomite was then proposed, and a chemical damage model of dolomite under dissolution was established. This investigation of the dolomite damage mechanism enriches the damage model of rocks under hydrochemical action and provides an important theoretical basis for the engineering production and scientific exploration of dolomite in dissolution environments.

## 2. Materials and Methods

### 2.1. Materials and Instruments

Fresh rock samples were selected in the tunnel. Combined with mineral identification and microstructure analysis, the fresh rock samples were screened twice, and the rock samples with better internal structure integrity were selected. In the laboratory, the rock is processed into a standard cylindrical mechanical specimen of  $50 \times 100$  mm by an automatic diamond machine. The test material is shown in Figure 1. The mass of rock samples was

measured using an electronic scale (precision 0.01 g), and the maximum and minimum values of mass were eliminated. The average density was  $2.7 \text{ g/cm}^3$ . The experimental group was treated with acid as sulfuric acid, and 1 hydrochloric acid group control test was used to compare and analyze the dissolution phenomenon. Solutions with different pH values were prepared for dissolution reaction. The mechanical test instrument and microscopic test instrument after reaction are shown in Figure 2.

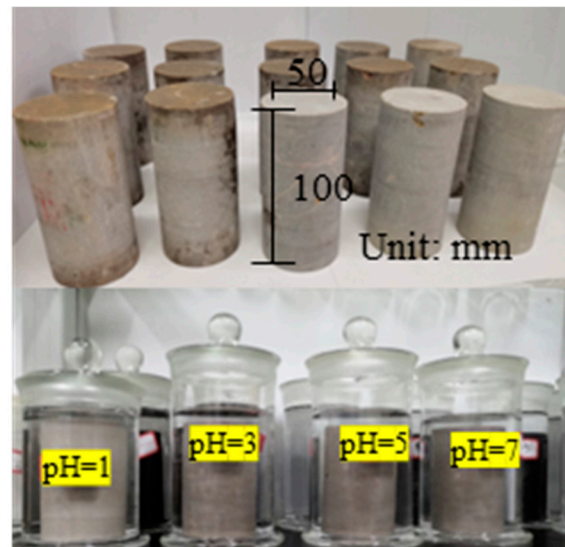


**Figure 1.** Dissolution test and standard mechanical specimen.

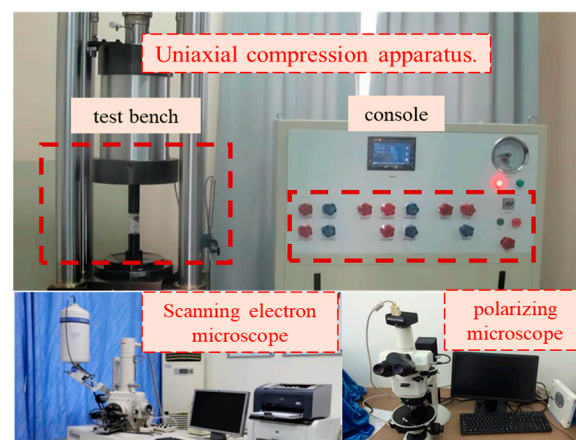


**Figure 2.** Uniaxial compression apparatus and scanning electron microscope. (Polarizing microscope Nikon LV100POL was used for polarizing microscope. Scanning electron microscope model is Quanta250 FEG. The rock mechanics test uses the YSJ-01-00 rock triaxial creep testing machine independently developed by the National Key Laboratory of Geological Disaster Prevention and Geological Environment Protection of Chengdu University of Technology.)

## 2.2. Dissolution Test

The waves velocity of rock samples was tested using a wave velocity tester. The wave velocity of each rock sample was close to each other, and the homogeneity of rock samples was good. Firstly, the dissolution test was carried out on the mechanical samples. The rock samples were placed in a closed glass container for dissolution. The pH was 1, 3, 5, and 7, respectively, and the solution was replaced every 3 days. After the dissolution test, the rock samples were placed in an electrothermal blast drying oven and dried at  $105 \text{ }^\circ\text{C}$  for 12 h. The dried rock samples were placed in a microcomputer hydraulic servo pressure testing machine for conventional compression tests. Firstly, a uniaxial compression test

was carried out. Because there was no confining pressure in the test, the test process was fast, and the uniaxial compression test can reflect the damage effect of dissolution on the internal structure of rock samples to a large extent.

### 2.3. Water Chemical Analysis

Numerous springs were present in the study area, and springs found throughout the upper, middle, and lower sections of the tunnel were investigated. Four characteristic spring water samples were collected nearby this area for water quality analysis (Figure 3). AquaChem was used to draw a three-line Piper diagram (Figure 4) to determine the quality of the water in this location. The Piper trilinear diagram comprises three parts. The triangles on the lower left and lower right represent the relative molar percentages of cations and anions, respectively. The intersection obtained by extending the diamond upwards represents the relative content of anions and cations in the water sample.



Figure 3. The characteristics of spring points in the study area.

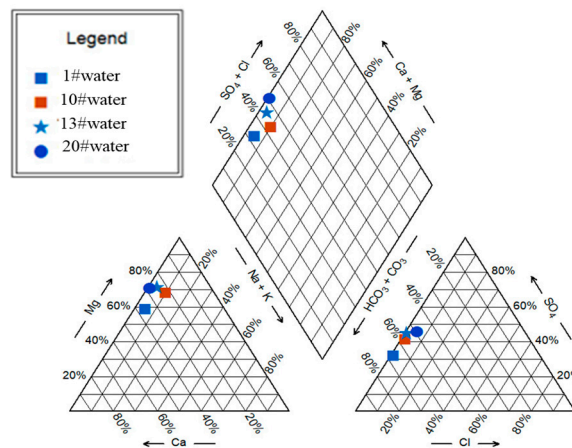
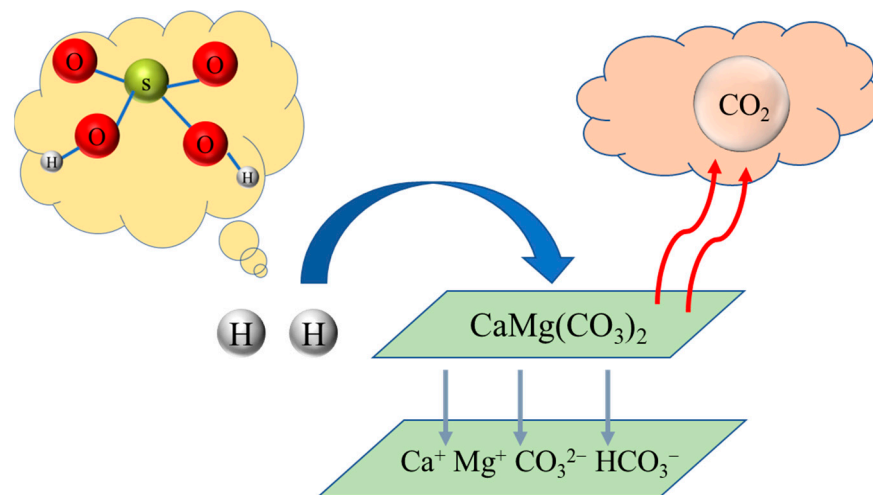


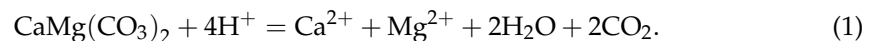
Figure 4. Piper diagram of spring points.

The water chemistry types in the study area were in the form of either  $\text{HCO}_3\text{-Ca-Mg}$  or  $\text{HCO}_3\text{-SO}_4\text{-Ca-Mg}$ . The salinity of the groundwater was generally high, the flow rate was relatively slow, sufficient water-rock interactions were present, and the ion concentration in the water was high. The chemical characteristics of the groundwater in this area were conducive to the dissolution of dolomite (Figure 5).

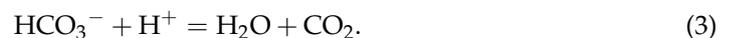
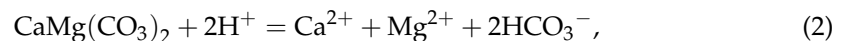


**Figure 5.** Chemical dissolution mechanism.

Through the study of chemical reaction conditions with experimental phenomena, it was concluded that when  $\text{pH} \leq 3$ , chemical dissolution is mainly based on the following formula:



When  $\text{pH} > 3$ , chemical dissolution is divided into the following two steps, and the first step reaction is the mainstay:



### 3. Results

#### 3.1. Dissolution Characteristics of Dolomite

At the same concentration, the reaction intensity of the rock sample in the hydrochloric acid group is greater than that in the sulfuric acid group, and the produced carbon dioxide causes number of bubbles in the container. When the reaction reached equilibrium, the two groups of solutions were relatively turbid. Among them, the hydrochloric acid group solution contains metal minerals, and trivalent iron is replaced in the reaction to synthesize ferric chloride so that the solution is khaki. The sulfuric acid group solution adsorbs some impurities due to the formation of calcium sulfate, making the solution white.

The surface of the rock sample dissolved under sulfuric acid conditions is relatively smooth when it is just taken out, and it is evenly covered with a layer of white dolomite sand. After washing and drying, the surface roughness of the rock sample is improved, but the overall dissolution phenomenon is weak. Under the condition of hydrochloric acid, yellow dolomite sand is locally attached to the surface.

The  $\text{CaSO}_4$  produced by the sulfuric acid group is slightly dissolved and attached to the surface of the rock sample, which hinders the reaction.  $\text{CaCl}_2$  produced under the condition of hydrochloric acid is soluble in water, and the reaction is less affected. However, due to the strong reaction, some products are still attached. Under the condition of hydrochloric acid, the dissolution is more intense, the surface fracture pores are very developed, some particles are attached and detached, and the roughness is obviously improved. The severity of the two groups of tests and the type of dolomite sand are shown in Figure 6.

The indoor dissolution phenomenon of the rock samples in the sulfuric acid group is compared with the field (Figure 7). The tunnel face is mostly white after weathering, and the generated karst products correspond to the white attachments on the surface of the rock samples in the indoor sulfuric acid group test. After dissolution, the rock samples of

the hydrochloric acid group produced multiple crisscrossed cracks on the surface, such as 'knife-cut' cracks. The 'knife-cut' corrosion morphology produced by the hydrochloric acid dissolution in the field can be seen (Figure 8).

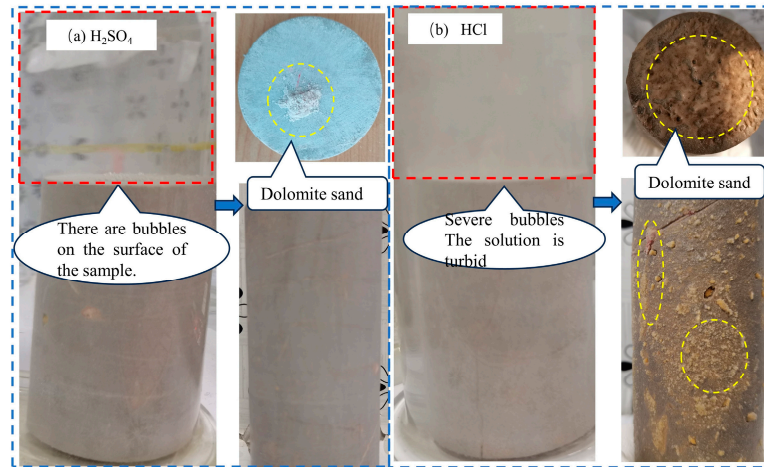


Figure 6. Characteristics of dolomite dissolution.

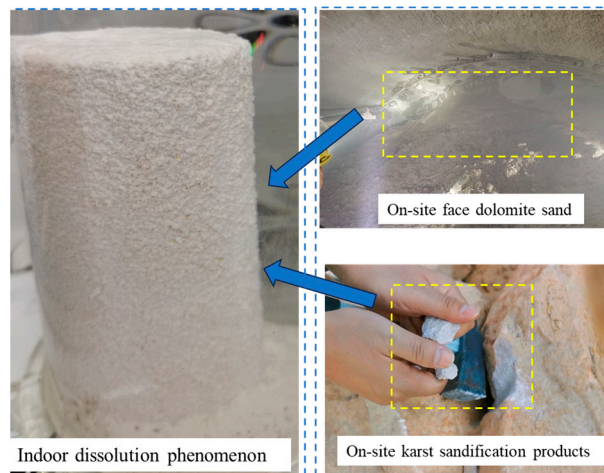


Figure 7. Contrast of corrosion phenomenon (sulfuric acid group).

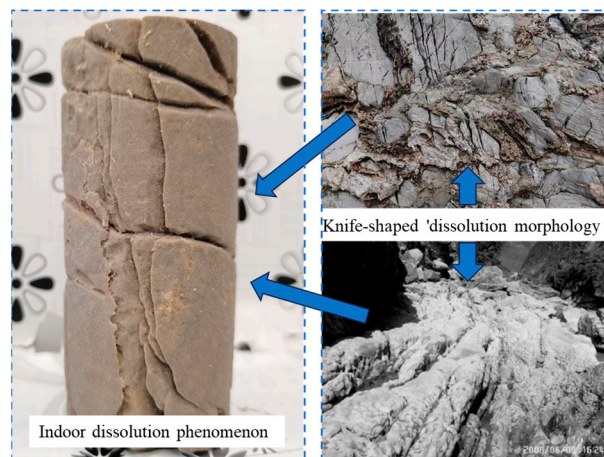
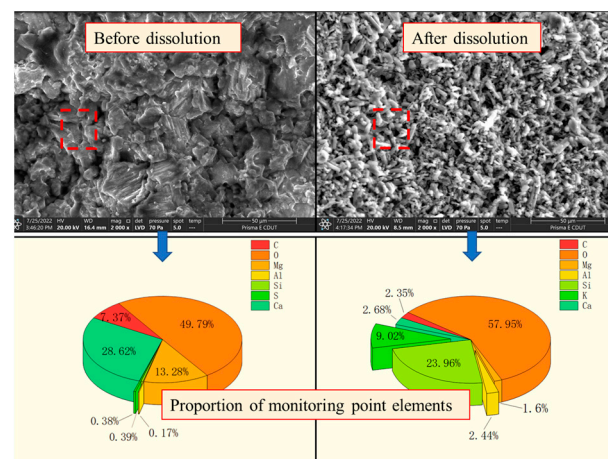


Figure 8. Corrosion phenomenon control (hydrochloric acid group).

### 3.2. Microstructure Evolution and Element Migration Change

Sliced samples with different dissolution times were removed for scanning electron microscopy analysis. Combined with the macroscopic dissolution characteristics, dolomite was found to be mostly dissolved along the intercrystalline pores and crystal junctions. During the dissolution process, the crystals often fall off to form dolomite powder. However, dolomite powder formation was not observed for the majority of the samples. During the dissolution process, the clay minerals contained in the samples were wrapped in dolomite crystals on the surface or within, and the crystals were not easily separated from the parent rock. Macroscopically, the rock still possessed a complete structure; however, it remained adequately delicate to be crushed manually. Combined with the EDS (Electronic Differential System) analysis, the EDS of the same point in the scanning map showed that the content of oxygen was stable during the dissolution process, while the content of C was stable during the initial dissolution. As the dissolution time increased, the C content was reduced by 71%, and the content of Mg and Ca displayed a similar trend, which were reduced by 87.9% and 90.6%, respectively. The carbonate composed of these elements gradually dissolved during the dissolution process, while oxygen supplementation occurred during the replacement process; the overall content therefore remained stable (Figure 9).



**Figure 9.** Scanning electron microscopy and EDS energy spectrum analysis.

### 3.3. Failure Characteristics

The uniaxial compression failure characteristics of the rock sample at pH = 1 are shown in Figure 10. Due to the strong acidity, the H<sup>+</sup> penetration ability is strong and the penetration is deep. The failure characteristics are as follows:

Under the failure mode 1 of the rock sample, due to the short dissolution time, H<sup>+</sup> has no sufficient infiltration time, so the fracture development of the rock sample is shallow under the action of external force, and finally the longitudinal fracture is destroyed along the three surfaces, and the cracks are connected.

Under the failure mode 2 of the rock sample, the main control cracks of the stress failure of the rock sample are still on the surface layer, and the main longitudinal penetrating cracks are still three. However, due to the strong acidity, H<sup>+</sup> partially infiltrates into the interior of the rock sample, which makes the internal pores partially penetrate, and develops another two transverse fissures between the longitudinal fissures and extends to the interior of the rock sample. The length is about 18 mm, causing the rock sample to fall off. The length of the falling rock sample is about 40 mm, and the width is about 18 mm. The joint development of longitudinal and transverse fissures further reduces the compressive strength of rock samples.

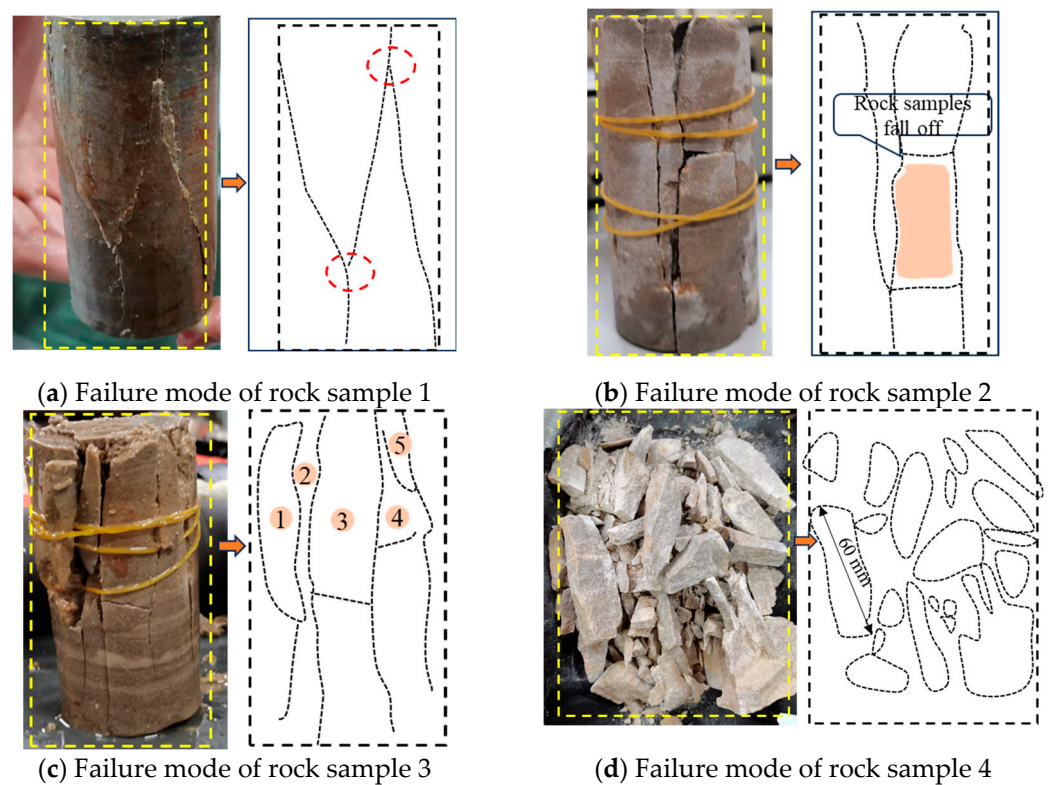


**Figure 10.** Mechanical failure characteristics of rock samples in pH = 1 test group.

Under the failure mode 3 of the rock sample,  $H^+$  further infiltrated into the rock sample, which improved the connectivity of the internal pores. When subjected to pressure, the longitudinal and transverse fissures are further developed. There are six main longitudinal fissures, and about three transverse fissures developed between them. The size is small, about 15~20 mm in length, and the rock samples fall off more, about five pieces, but mainly the surface layer falls off and the thickness is small.

Under the failure mode 4 of the rock sample, a large amount of  $H^+$  infiltrated into the rock sample, and many mineral crystals inside the rock sample were dissolved and destroyed. The connectivity between pores is enhanced, and the horizontal and vertical cracks are developed from the surface to the inside. The cracks are connected to each other and the size is large. Under the action of external force, the compressive strength of dolomite crystal minerals is greatly reduced due to corrosion damage, and finally the rock sample is disintegrated and destroyed. At the end of the test, the rock samples could not be completely taken out, and the rock samples were dispersed into blocks of different sizes. The maximum block length was about 60 mm, and the width was about 20 mm.

#### 4. Discussion

##### 4.1. Analysis of Dissolution Effect on Microstructure Damage

The dolomite in the study area was primarily of high purity (greater than 96%). The test samples were identified as fine-powder crystalline dolomite using thin sections. The particle sizes ranged from 0.02 to 0.04 mm. Combining the macroscopic dissolution characteristics of the mechanical specimens to establish a dolomite model composed of a spherical fine powder crystal dolomite crystal arrangement (Figure 11), the model was divided into three zones: the dissolution (dolomite), insoluble, and pore areas. The ratio of the dolomite crystal volume to the sample volume was greater than  $10^{-10}$ . Therefore, dolomite crystals were assumed to completely fill the dissolution zone.

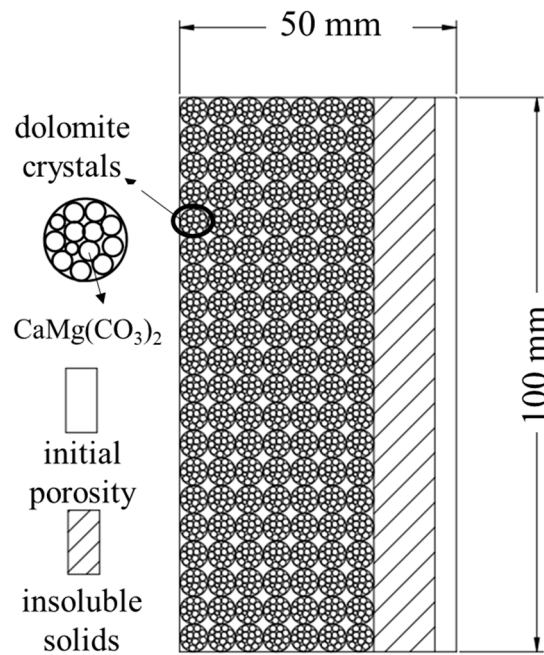


Figure 11. Hypothetical rock microscopic composition.

The dissolution zone of the dolomite samples was assumed to be composed of dolomite crystals. The dolomite crystals were composed of several  $\text{CaMg}(\text{CO}_3)_2$  molecules. Using scanning electron microscopy, the microscopic damage to the sample was divided into the destruction of dolomite crystals and crystal shedding caused by the dissolution of dolomite crystals, which manifested as the loss of dolomite crystals during the chemical reaction.

These two types of dissolution damage manifested as an increase in dolomite pores. The damaged porosity of the ideal rock after full dissolution using an acid solution with a pH of  $n$  is represented by  $\varphi_1$ . With the initial pore  $\varphi_0$  of the sample, the porosity of the model after damage is represented by  $\varphi_n$  (Equation (4)).

$$\varphi_n = \varphi_0 + \varphi_1 \tag{4}$$

The intracrystalline damage of the dolomite crystal was caused by the layer-by-layer shedding of the crystal surface. The development of intergranular dissolved pores was also indirectly caused by grain damage. The model exhibited damage to the crystal radius. The microdolomite crystal damage radius  $R(t)$  was defined according to the macrosandstone dissolution immersion depth proposed by Zhou J.F [24]. The specific solution process is as follows ( $t > 0$ ):

$$R(t) = |a \ln(t)| + b \tag{5}$$

$$V' = \frac{4}{3}\pi[R - R(t)]^3 \tag{6}$$

where  $t$  is the dissolution time,  $R$  is the initial particle size of the dolomite crystal,  $V'$  is the volume of a single dolomite crystal after damage, and  $a$  and  $b$  are parameters determined by rock properties, temperature, acidity, and other factors.

The number of damaged crystals was related to the mass of  $\text{CaMg}(\text{CO}_3)_2$  involved in the chemical reaction. Ideally, the chemical reactions that should occur in the samples are as Equation (1).

The comprehensive reaction rate  $V_{H^+}$  of  $H^+$  can be obtained by the following chemical reaction:

$$V_{H^+} = \lambda C_{H^+}^y \tag{7}$$

where  $\lambda$  is the comprehensive reaction rate parameter,  $C_{H^+}^y$  is the instantaneous concentration of  $H^+$  at a particular time, and  $y$  is the reaction order [20].

Therefore,

$$-\frac{dC_{H^+}}{dt} = \lambda C_{H^+}^y \tag{8}$$

According to the solution of the first-order linear differential equation and initial conditions of the reaction concentration, the relationship between the  $H^+$  concentration and time can be obtained as follows:

$$C_{H^+}^t = \left[ (C_{H^+}^0)^{1-x} - (1-x)\lambda t \right]^{\frac{1}{1-x}} \tag{9}$$

where  $C_{H^+}^0$  is the initial concentration of the chemical solution at a certain time. Because the following relationship exists,

$$pH = -\lg C_{H^+} \tag{10}$$

Equations (9) and (10) could be combined to produce the following relationship of solution pH versus time:

$$pH(t) = -\lg \left[ (10^{pH_0^{(x-1)}} + (x-1)\lambda t) \right]^{\frac{1}{1-x}} \tag{11}$$

By simulating the change in different  $pH$ , the modeled data could accurately simulate the experimental data (Figure 12). The  $x$  and  $\lambda$  parameters can be obtained according to the curve-fitting results of the relationship between the  $pH$  value and rock soaking time, which are 1.23 and 3.40, respectively.

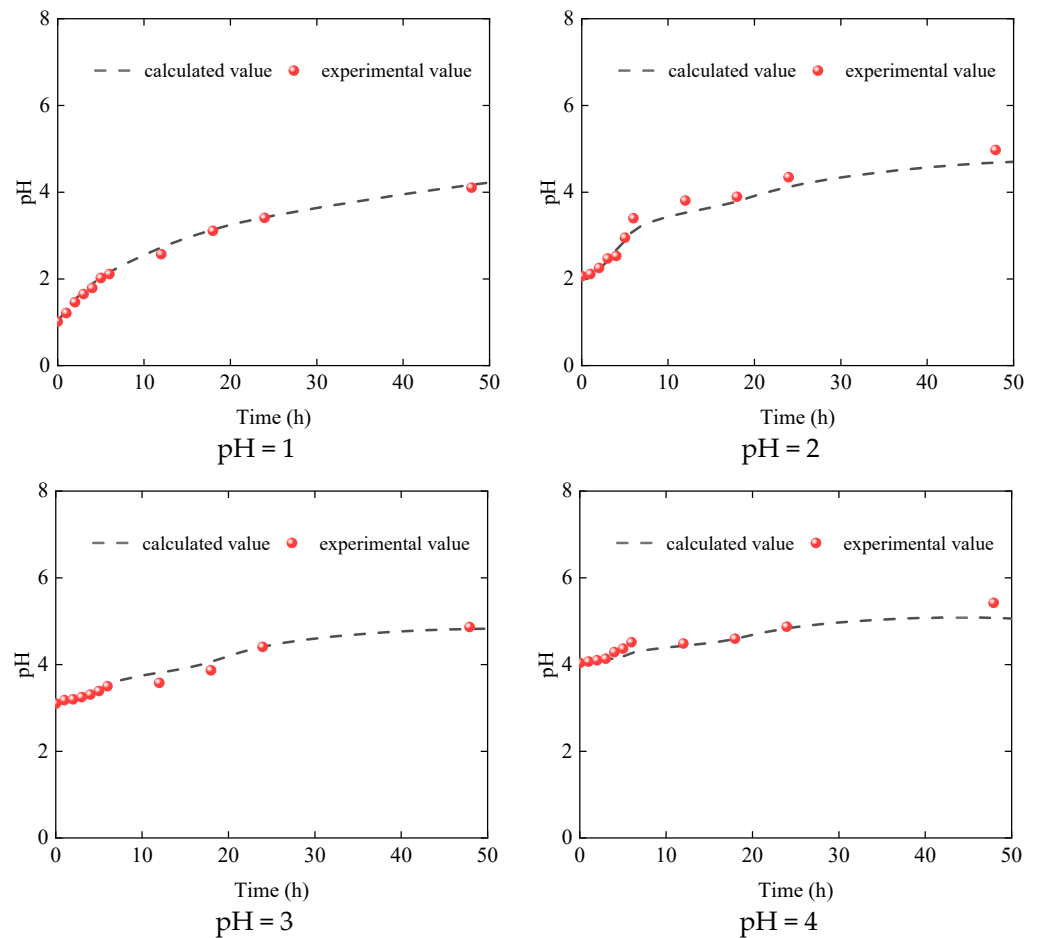


Figure 12. Comparison of pH value simulation results with experimental data.

According to the principle of chemical reaction,

$$n_t = 0.25 \times (C_{H^+}^0 - C_{H^+}^t) \times V_s \tag{12}$$

where  $n_t$  is the mass of the  $\text{CaMg}(\text{CO}_3)_2$  consumed during the reaction and  $V_s$  is the initial volume of acid solution. According to Equations (10) and (11), when the pH and volume of the solution are known, the mass of  $\text{CaMg}(\text{CO}_3)_2$  molecules can be consumed.

In this study, the amount of damage to dolomite crystals is related to the consumption  $n_t$  of  $\text{CaMg}(\text{CO}_3)_2$  molecules in the chemical reaction.  $k_1$  is the equivalent parameter of the conversion between the molecular weight consumed and the number of damaged dolomite crystals. The final dolomite crystal damage porosity  $\varphi_{n1}$  is the ratio of the volume damage  $V'$  of a single dolomite crystal to the mass  $n_t$  of the  $\text{CaMg}(\text{CO}_3)_2$  molecule consumed in the reaction process, and the product of the equal parameter  $k_1$  between the two and the initial volume  $V_0$  of the sample. Finally, the damage-pore expression of the dolomite model is given by Equation (13):

$$\varphi_{n1} = \frac{V'k_1n_t}{V_0} \tag{13}$$

$$\varphi_{n1} = \frac{\pi k_1 V_s \times [R - (|a \ln(t)| + b)]^3 \times (C_{H^+}^0 - [(C_{H^+}^0)^{1-x} - (1-x)\lambda t]^{\frac{1}{1-x}})}{3V_0} \tag{14}$$

#### 4.2. Strength Degradation and Evolution Model of Dolomite

Diluted sulfuric acid was used as the acid solution.  $\text{H}^+$  ionized from dilute sulfuric acid reacted with the  $\text{CaMg}(\text{CO}_3)_2$  molecules in the sample. The molecular structure was destroyed, the dolomite crystal structure was unstable, and pores developed. The connection between the pores produces microcracks. As the reaction proceeded, some microfractures were penetrated. When subjected to external forces, the fractures develop further in the dominant direction. The fractures developed further in the dominant direction. The indoor dissolution damage mode of dolomite is illustrated in Figure 13.

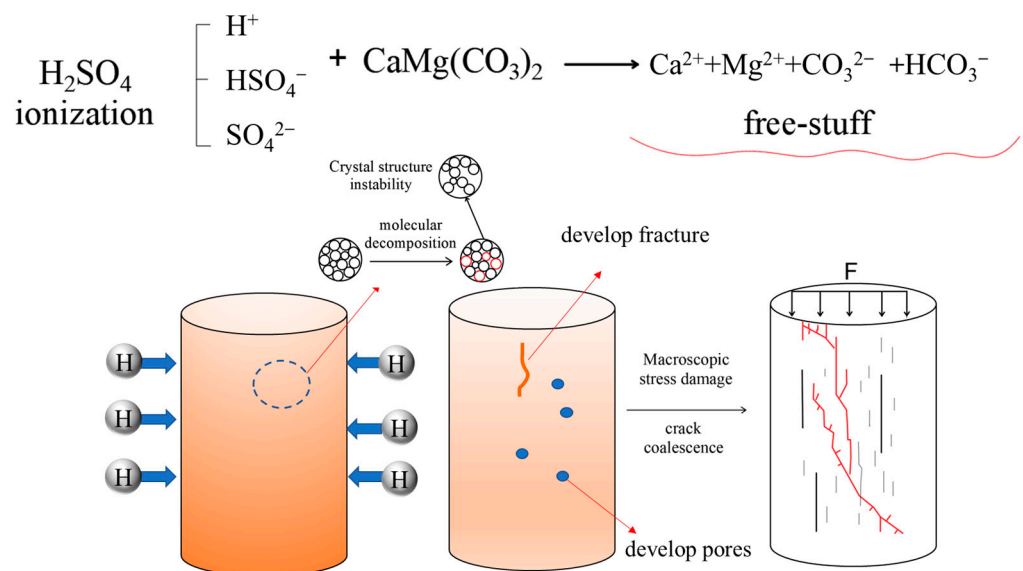


Figure 13. Damage model damage simulation.

Based on the previous analysis, dolomite dissolution damage was determined by monitoring the pH changes, and the pore damage was characterized. Based on the damage variable defined by the porosity change before and after dissolution [25], combined with the

damage model proposed in this study based on the dissolution characteristics of dolomite, the chemical damage to dolomite was defined as  $D_C$ .

$$D_C = 1 - \frac{1 - \varphi_n}{1 - \varphi_0} \quad (15)$$

The damage theory is based on chemical kinetics. The metathesis reaction between  $H^+$  in the acid solution and dolomite crystals played a major role in the dolomite dissolution process. Metathesis is a reaction in which two compounds exchange components to form two other compounds. The two compounds of the metathesis reaction exchanged ions in the reaction system (mostly aqueous solution) combined with precipitation, gas, or weak electrolytes (most commonly water) that were difficult to ionize. The ion concentration in the reaction system was reduced, and the chemical reaction was carried out in the direction of ion concentration reduction. The concept of reaction order proposed by the American chemist Noyce Hou et al. [26] was introduced to determine the  $H^+$  consumption related to the reaction.

Based on the chemical damage model [14], a damage variable based on  $H^+$  consumption was established. The equivalent damage stress of dolomite after the dissolution was established according to the generalized Lemaitre strain equivalence principle [27].  $\sigma_0$  is the uniaxial compressive strength of the sample without dissolution. Finally, the uniaxial compressive strength  $\sigma$  of dolomite after chemical damage is as follows:

$$\sigma = (1 - D_c)\sigma_0 \quad (16)$$

#### 4.3. Model Verification

Under ideal conditions, when the acidic solution is sufficient, the soluble matter would react completely regardless of the pH value, which is a time-scale problem. The limit operation results of the damage formula showed that under the strongest level of acidity (pH = 1), the theoretical dissolution time of the hypothetical rock was 1640 h, which was longer than the experimental value of 504 h; therefore, the model was applicable to the entire dissolution process. The data from the damage model are listed in Table 1.

**Table 1.** Basic data of samples.

Essential Parameter	Values
Original porosity $\varphi_0/\%$	4.28
Crystal size R/mm	0.03
Initial acid solution volume $V_s/L$	0.8
Initial volume of specimen $V_0/m^3$	$1.96 \times 10^{-4}$
Single axis compressive strength $\sigma_0/MPa$	78.6
Grain volume $V/m^3$	$1.62 \times 10^{-13}$

The indoor dissolution test of dolomite showed that the dissolution mechanism was the same under different pH conditions, but the dissolution rate was faster and the rock damage was greater in a low-pH environment, which was manifested as a change in model parameters. According to the monitoring data of the indoor dissolution time and model data, the following parameters were obtained (Table 2).

**Table 2.** Values of different pH parameters.

Parameter	pH = 1	pH = 3	pH = 5	pH = 7
k	1.26	0.611	0.03	0.02
a	0.0025	0.004	0.013	0.012
b	0.00729	0.0012	−0.0158	−0.01

The dissolution amount of rock samples under different dissolution times can be obtained from the chemical reaction rate equation. The pore damage amount of rock samples can be obtained by substituting it into the damage model, and the chemical damage ( $D_c$ ) can then be obtained. Finally, the strength predicted by the chemical damage model in this study was calculated, and the fit with the experimental value is shown in Figure 14.

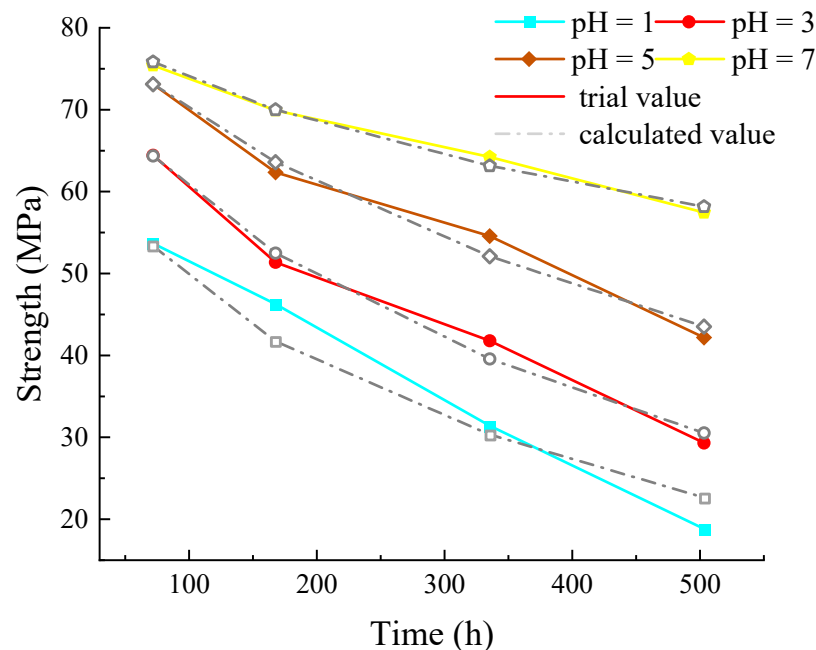


Figure 14. Strength-fitting curve.

The comparison between the model and experimental values proposed in this study showed that the proposed chemical damage model displayed good prediction accuracy and reliability in the process of a short-term dolomite indoor dissolution test. The rate of dissolution decreased with time, mainly because of the physical effects of water. However, the model in this study was suitable for a time scale dominated by chemical dissolution, and was applicable to certain time conditions. Subsequently, a time scale that decayed with the dissolution time could be defined according to the relationship between the pore damage of rock samples at different pH values proposed by the model, and the application scope of the model could be improved.

## 5. Conclusions

In this study, dolomite affected by a variety of hydrochemical solutions was investigated. Based on the dissolution characteristics of dolomite as the background and the dissolution law obtained from the dolomite indoor dissolution test, in addition to the results from the microscopic analysis, we defined an idealized model consistent with dolomite dissolution damage. Based on damage theory and the dolomite chemical damage model, the following conclusions were obtained:

(1) The dissolution degree of dolomite in the study area under the sulfuric acid environment is less than that under the hydrochloric acid environment. The dissolution under sulfuric acid mostly produces the phenomenon of 'sand inclusion', and the dissolution under hydrochloric acid mostly produces the phenomenon of 'knife cutting'. The failure characteristics of rock samples after corrosion are mainly as follows: from the development of longitudinal cracks to the joint development between transverse and longitudinal cracks. As the corrosion progresses,  $H^+$  penetrates into the rock sample to participate in the reaction, and the cracks also develop into the rock sample. Inside, the broken rock blocks increase when the force is destroyed.

(2) Dolomite dissolution mainly manifested as dolomite crystal damage. Based on monitoring pH changes, pore damage was characterized by the deduced dolomite chemical damage formula. The fitting degree was greater than 98%, and the model could better simulate the strength damage of dolomite under dissolution conditions.

(3) The damage model proposed in this study can not only simulate the strength attenuation caused by chemical damage, but can also be used as the basis for studying the pore damage in dolomite dissolution and the time scale under different dissolution environments, providing a theoretical basis for the multi-angle study of dolomite dissolution.

(4) This model is suitable for high-purity and low-porosity dolomite, but is not suitable for low-purity and high-porosity dolomite.

**Author Contributions:** Conceptualization, W.L.; methodology, F.J.; writing, P.L.; resources, H.X.; investigation, X.M. All authors have read and agreed to the published version of the manuscript.

**Funding:** This research was funded by National Natural Science Foundation of China program No. 41977237.

**Data Availability Statement:** Data are contained within the article.

**Acknowledgments:** The valuable comments made by the all anonymous reviewers are sincerely consented.

**Conflicts of Interest:** Wenlian Liu was employed by the company Kunming Prospecting Design Institute of China Nonferrous Metals Industry. The remaining authors declare that the research was conducted in the absence of any commercial or financial relationships that could be construed as a potential conflict of interest.

## References

1. Zhang, L.X.; Zhao, Q.H.; Hu, X.B.; Han, G.; Zhao, X. Laboratory dissolution test on dolomite and its microdissolution mechanism. *J. Eng. Geol.* **2012**, *20*, 576–584.
2. Xiao, F.K.; Wang, H.R.; Liu, G.; Yin, P.S.; Hou, Z.Y.; Cheng, Q.L.; Zhao, W.H. Study on the whole process model of rock creep considering damage factors. *Coal Sci. Technol.* **2021**, *49*, 322–327.
3. Liu, Q.; Bai, Y.E.; Gu, Z.F.; Lu, Y.R.; Sheng, Z.P. Experimental study on dissolution-creep characteristics of limestone and dolomite in rocky desertification area—A case study of Zhenfeng-Guanling Huajiang karst area in Guizhou. *J. Guilin Univ. Technol.* **2017**, *37*, 399–404.
4. Gautelier, M.; Schott, J.; Oelkers, E.H. An experimental study of dolomite dissolution rates at 80 °C as a function of chemical affinity and solution composition. *Chem. Geol.* **2007**, *242*, 509–517. [[CrossRef](#)]
5. Tang, L.S.; Wang, S.J. Discussion on mechanism and quantification method of chemical damage of rock water. *J. Rock Mech. Eng.* **2002**, *3*, 314–319.
6. Wang, W.; Liu, T.G.; Lv, J.; Wang, R.B.; Xu, W.Y.; Jian, B. Experimental study of influence of water-rock chemical interaction on mechanical characteristics of sandstone. *J. Rock Mech. Eng.* **2012**, *31*, 3607–3617.
7. Tang, Y.C.; Fang, J.N.; Zhou, H. Experimental study of rock salt dissolving characteristics under triaxial stress. *Rock Soil Mech.* **2012**, *33*, 1601–1607.
8. Wei, X.H.; Ma, T.T.; Wang, J.; Ye, H.Z. Simulation study on the effect of aqueous solution with different pH values on the dissolution of limestone. *J. Foshan Univ.* **2013**, *31*, 17–23.
9. Tian, W. Experimental simulation of dissolution process of the Lower Paleozoic carbonate rocks in Zhuanghai Area under supergene conditions. *Acta Mineral. Sin.* **2019**, *39*, 108–116.
10. Li, S.; Huo, R.; Yoshiaki, F.; Ren, D.; Song, Z. Effect of acid-temperature-pressure on the damage characteristics of sandstone. *Int. J. Rock Mech. Min. Sci.* **2019**, *122*, 104079. [[CrossRef](#)]
11. Liu, W.; Liu, P.; Xu, H.; Gong, B.; Ji, F. Study on the Microstructure Evolution and Strength Damage Mechanism of Dolomite under Dissolution Condition. *Sustainability* **2022**, *14*, 11447. [[CrossRef](#)]
12. Xie, S.Y.; Shao, J.F.; Xu, W.Y. Influences of chemical degradation on mechanical behaviour of a limestone. *Int. J. Rock Mech. Min. Sci.* **2011**, *48*, 741–747. [[CrossRef](#)]
13. Miao, S.; Wang, H.; Cai, M.; Song, Y.; Ma, J. Damage constitutive model and variables of cracked rock in a hydro-chemical environment. *Arab. J. Geosci.* **2018**, *11*, 19. [[CrossRef](#)]
14. Li, N.; Zhu, Y.M.; Zhang, P.; Ge, X.R. A chemical damage model of sandstone in acid environment. *Chin. J. Geotech. Eng.* **2003**, *4*, 395–399.
15. Chen, S.L.; Feng, X.T. Study on triaxial meso-failure mechanism and damage variables of sandstone under chemical erosion. *Geotechnical mechanics. Geotech. Mech.* **2004**, *9*, 1363–1367.

16. Ding, W.X.; Feng, X.T. Testing study on mechanical effect for limestone under chemical erosion. *Chin. J. Rock Mech. Eng.* **2004**, *21*, 3571–3576.
17. Qiao, L.P.; Liu, J.; Feng, X.T. Study on damage mechanism of sandstone under hydro-physico-chemical effects. *Chin. J. Rock Mech. Eng.* **2007**, *10*, 2117–2124.
18. Liu, J.; Li, J.L.; Zhang, Y.D.; Qu, J.J.; Chen, X.; Qin, Y.H. Study of time scale and strength model of yichang sandstone under different ph values of acidic solution immersion. *J. Rock Mech. Eng.* **2010**, *29*, 2319–2327.
19. Deng, H.F.; Hu, A.L.; Li, J.L.; Zhang, X.J.; Hu, Y.; Chang, D.L.; Zhu, M. Statistical damage constitutive model of sandstone under water-rock interaction. *Rock Soil Mech.* **2017**, *38*, 631–639.
20. Feng, X.W.; Wang, W.; Wang, R.B.; Yuan, S.S.; Zhu, Q.Z. Ontogenetic model of rheological damage in sandstone considering water chemical damage. *Rock Soil Mech.* **2018**, *39*, 3340–3346+3354.
21. Zhu, C.; Xu, X.; Liu, W.; Xiong, F.; Lin, Y.; Cao, C.; Liu, X. Softening Damage Analysis of Gypsum Rock With Water Immersion Time Based on Laboratory Experiment. *IEEE Access* **2019**, *7*, 125575–125585. [[CrossRef](#)]
22. Lin, Y.; Gao, F.; Zhou, K.; Gao, R.; Guo, H. Mechanical Properties and Statistical Damage Constitutive Model of Rock under a Coupled Chemical-Mechanical Condition. *Geofluids* **2019**, *2019*, 7349584. [[CrossRef](#)]
23. Kuva, J.; Sammaljärvi, J.; Parkkonen, J.; Siitari-Kauppi, M.; Lehtonen, M.; Turpeinen, T.; Timonen, J.; Voutilainen, M. Imaging connected porosity of crystalline rock by contrast agent-aided X-ray microtomography and scanning electron microscopy. *J. Microsc.* **2018**, *270*, 98–109. [[CrossRef](#)] [[PubMed](#)]
24. Zhou, J.F. Study on prediction model for rock immersion time scale and deterioration under effect of acidic solution. *Water Resour. Hydropower Eng.* **2021**, *52*, 162–171.
25. Chen, Y.L.; Chen, Q.J.; Xiao, P.; Du, X.; Wang, S.R. Rock chemical corrosion-confining pressure damage constitutive model and discrete element simulation. *Chin. J. Solid Mech.* **2022**, *43*, 703–715.
26. Hou, W.H. An Outline of the Establishment and Development of Chemical Kinetics. *Univ. Chem.* **2007**, *3*, 28–36+66.
27. Zhang, Q.S.; Yang, G.S.; Ren, J.X. New study of damage variable and constitutive equation of rock. *Chin. J. Rock Mech. Eng.* **2003**, *1*, 30–34.

**Disclaimer/Publisher’s Note:** The statements, opinions and data contained in all publications are solely those of the individual author(s) and contributor(s) and not of MDPI and/or the editor(s). MDPI and/or the editor(s) disclaim responsibility for any injury to people or property resulting from any ideas, methods, instructions or products referred to in the content.